

# Analyzing limits for in-context learning

Omar Naim

IRIT France

omar.naim@irit.fr

Nicholas Asher

IRIT France

nicholas.asher@irit.fr

## Abstract

We examine limits of in-context learning (ICL) in transformer models trained from scratch, focusing on function approximation tasks as a controlled setting to uncover fundamental behaviors. While we show empirically that transformer models can generalize, approximating unseen classes of polynomial (non linear) functions, they cannot generalize beyond certain values. We provide both empirical and mathematical arguments explaining that these limitations stem from architectural components, namely layer normalization and the attention scoring function, softmax. Together, our findings reveal structural constraints on ICL that are often masked in more complex NLP tasks but that need to be understood to improve robustness and interpretability in transformer-based models.

## 1 Introduction

In-context learning (ICL) (Brown et al., 2020) is an emergent capability of large language models (LLMs), enabling them to learn a task from an instructional prompt and a few examples at inference time, without any modification of the model’s parameters from pretraining. Thus we can use LLMs without the computational and resource-intensive demands of pretraining or fine-tuning, challenging conventional distinctions between training and inference. ICL’s effectiveness has led to the adoption of LLMs in many applications.

While theoretical research has focused on what these models can learn in context, little attention has been devoted to understanding the inherent limitations of ICL. We study here ICL’s structural constraints and failure modes.

Understanding ICL mechanisms, which involve prompting and pretraining, requires precise control of experimental conditions. We study ICL in a well-defined setting using clean, structured data: our task is to in-context learn polynomial

functions. These mathematical problems are well-suited for analyzing ICL due to their structured and predictable nature. We explore the ICL task on functions in  $\mathbb{R}^n[X]$  for  $1 \leq n \leq 6$ , using a variety of training and testing distributions and a variety of transformer models. We examine the impact of architectural components such as feedforward layers and normalization, and conduct ablation experiments to understand the role of specific components in ICL.

Our main results and organization are as follows. After related work and background sections, Section 4 details the experimental set up and shows that small transformer models with attention only architectures are both necessary and sufficient for ICL of several classes of polynomial functions, even classes whose class forms they did not encounter in training, as well as some continuous functions. This shows a generalization capacity across function classes, and the primacy of attention in our task reflects prior work on the importance of attention layers in NLP tasks.

However, Section 5 shows that our models fail to generalize their predictions for all functions  $f$  and inputs  $x$ , where  $x, f(x)$  lie outside the training distributions. Section 6 provides a mathematical expression of the ICL problem and gives a derives generalization failures from normalization and scoring functions. This highlights a fundamental dilemma. On one hand, the normalization layer restricts the model’s ability to generalize beyond certain input ranges. On the other hand, while removing normalization unexpectedly improves performance in our setting, if the query input has a high embedding norm, the model’s output diverges toward a linear function determined mainly by its parameters fixed in pretraining, effectively precluding ICL. This reveals a distinct failure mode of ICL in the high-norm regime, both in the presence, and absence, of normalization. But the attention scoring function itself also introduces structural

limitations that hinder the model’s ability to leverage contextual information. Taken together, these results suggest that generalization failures in ICL stem from a transformer’s basic architectural design. To alleviate some of these problems, we suggest constraining embedding functions to avoid high-norm vectors and reduce variability in weight magnitudes.

Focusing on well-defined and structured mathematical problems with deterministic answers enables us to avoid many subtleties of prompt engineering and of managing the large scale pretraining involved in language tasks. We can more easily and confidently measure a model’s ability to generalize, recognize patterns and reason from a few examples. The consistent patterns within polynomial functions, such as the relationship between degree and curvature for instance, make them ideal for testing whether models are truly grasping mathematical relationships rather than just memorizing specific instances. Our findings are thus applicable to ICL tasks in general. We briefly discuss consequences for NLP in the last section.

## 2 Related Work

(Brown et al., 2020) introduced in-context learning (ICL) as a framework that occurs entirely at inference time; LLMs learn tasks by analogy based on examples presented in the prompt without updating their parameters. Despite its promise, the underlying mechanisms behind ICL remain only partially understood.

(Akyürek et al., 2022; Von Oswald et al., 2023; Fu et al., 2023; Xie et al., 2021; Wu et al., 2023; Zhang et al., 2023; Panwar et al., 2023) have suggested that LLMs perform implicit gradient-based updates, higher-order optimization, or approximate Bayesian inference when prompted with in-context examples. However, these remain speculative hypotheses grounded in what the architecture could, in principle, implement, rather than direct evidence of the mechanisms at play. As noted by (Dong et al., 2022), much of this analysis remains confined to simple tasks, such as linear regression or Boolean functions (Bhattamishra et al., 2023).

(Garg et al., 2022) showed that small transformers trained from scratch on synthetic data can acquire ICL abilities, providing early evidence that ICL is not solely a consequence of model size pretraining on language, but a trainable capability. Similarly, Raventós et al. (2024) studied how ICL

performance changes as a function of the number of pretraining examples.

(Olsson et al., 2022) investigated architectural components responsible for ICL, proposing that *induction heads*, a learned copying and comparison mechanism, underlie ICL. (Geva et al., 2021) and (Bietti et al., 2024) explored the role of memory in transformers, showing that models heavily rely on memorization via attention matrices. This is further supported by findings from (Yu et al., 2023) and (Geva et al., 2023), who argue that transformers prioritize memorized patterns during inference.

(Naim and Asher, 2024) showed that transformers trained from scratch on linear functions fail to extrapolate, when evaluated out of distribution: performance degrades from accurate prediction, to constant outputs, to near-random behavior, introducing the notion of *boundary values*.

## 3 Training for In-context learning

### 3.1 Learning in-context

Learning a task in-context means that the model is able to predict the output for a new input using only a few input-output examples provided within the same sequence. Specifically, given a prompt of few input-output examples of the form  $(x_1, g(x_1), \dots, x_p, g(x_p), x)$ , a transformer is able to approximate the value of  $g(x)$ , regardless of which specific input samples  $x_i$  are included in the in-context examples.

We distinguish two notions of "learning a class of functions in context". The first, call it  $ICL_1$ , states that a transformer model  $\hat{f}^\theta$  can ICL a function class  $\mathcal{F}$  on a given distribution sampling functions  $g \in D_{\mathcal{F}}$  and a distribution matching inputs  $x_i \in D_{\mathcal{I}}$  where both correspond to training distribution:

$$\forall x_i, y_i, x \in D_{\mathcal{I}} \forall g \in D_{\mathcal{F}}, \quad (1)$$

$$\|\hat{f}^\theta(x_1, g(x_1), \dots, x_p, g(x_p), x) - g(x)\|^2 \approx$$

$$\|\hat{f}^\theta(y_1, g(y_1), \dots, y_p, g(y_p), x) - g(x)\|^2 < \epsilon$$

A second definition of ICL is more restrictive: a model  $M$  can  $ICL_2$  a function class  $\mathcal{F}$  if it is capable of approximating all functions within the target class across all possible distributions over functions and inputs.

### 3.2 Loss function

Training<sup>1</sup> a model to perform in-context learning can be seen as meta-learning (Schmidhuber et al., 1996) where the model learns to perform new tasks based on in-context examples, without any changes on its parameters. In practice, for autoregressive models, the ICL objective is implemented through standard supervised learning (Brown et al., 2020; Garg et al., 2022; Akyürek et al., 2022): the model is presented with multiple functions from a given class, each evaluated at several input points, and is trained to learn the underlying function class.

Our ICL tasks involve training from scratch on sequences containing in-context examples (input-output pairs)  $(x_1, f(x_1), \dots, x_i)$  ending with a query input  $x_i$  that is used to generate the corresponding output. We train a transformer model  $f^\theta$  parameterized by  $\theta$  to minimize the expected ICL loss over all the prompts:

$$\min_{\theta} \mathbb{E}_{g \sim \mathcal{D}_{\mathcal{F}}} \left[ \mathbb{E}_{x_1, \dots, x_p \sim \mathcal{D}_{\mathcal{I}}} \sum_{i=0}^k \ell(y_{i+1}, f^\theta((x_1, g(x_1), \dots, x_{i+1}))) \right] \quad (2)$$

where  $\ell(.,.)$  represents the squared error and  $g \sim \mathcal{D}_{\mathcal{F}}$  a polynomial function  $g : x \mapsto \sum_{i=0}^n a_i x^i$ , with weights  $\forall i \in 1, \dots, n$   $a_i \sim \mathcal{D}_{\mathcal{F}}$ . Samples  $x_i$  are picked randomly according to a training distribution for points  $\mathcal{D}_{\mathcal{I}}$  (see Appendix A for more details). We employ curriculum learning on a set  $S$  of training sequences of varying lengths, ranging from 1 to  $k = 40$ . Models are trained for 500k steps and use a batch size of 64, using Adam optimizer. The models saw over 1.3 billion training examples for each distribution we studied.

### 3.3 Evaluation metric

We evaluated the model’s generalization capabilities across a range of testing distributions for both functions, denoted  $\mathcal{D}_{\mathcal{F}}^{test}$  and input data points, denoted  $\mathcal{D}_{\mathcal{I}}^{test}$ .

For each testing scenario  $(\mathcal{D}_{\mathcal{I}}^{test}, \mathcal{D}_{\mathcal{F}}^{test})$ , we generate a set of  $N = 100$  functions sampled from  $\mathcal{D}_{\mathcal{F}}^{test}$ . For each function we sample  $N_b = 64$  batches, where each batch contains  $N_p = 41$  data points drawn from  $\mathcal{D}_{\mathcal{I}}^{test}$ . Within each batch  $b$ , we predict output of prompts

$(x_1^b, f(x_1^b), \dots, x_{k-1}^b, f(x_{k-1}^b), x_k^b)$  with  $k \geq 2$ . The mean squared error (MSE) is computed over all predictions within each batch and averaged across all batches for a given function. Finally, we report the overall ICL evaluation metric as the average MSE across the entire set of test functions.

$$\epsilon_{\sigma} = \frac{1}{N} \sum_{i=1}^N \sum_{b=1}^{N_b} \frac{1}{N_b} \left( \frac{1}{N_p} \sum_{i=3}^{N_p} (\text{pred}_i^b - y_i^b)^2 \right) \quad (3)$$

To improve interpretability of squared error values, we define *error rate*  $r_{\epsilon} = \frac{\epsilon_{\sigma}}{|\epsilon_{*} - \epsilon_0|}$  where  $\epsilon_{*}$  is the best  $\epsilon_{\sigma}$  error for a model  $M$  with  $\hat{f}(x)$  calculated with Least Squares, and  $\epsilon_0$  is the worst  $\epsilon_{\sigma}$  error for a model  $M$  such that  $\forall x, \hat{f}_M(x) = 0$ . In all our error calculations, we exclude the first  $n + 1$  predictions of each batch from the squared error calculation for  $g \in \mathbb{R}^n[X]$ , since we need at least  $n+1$  points to be able to find  $g$ .

To ensure fair and meaningful comparisons across models, we fix the random seed when generating the 100 test functions and the corresponding prompting points  $x_i$ . This guarantees that all models are evaluated on the same set of functions and input distributions. The purpose of this evaluation setup is to assess how well models generalize when progressively exposed to out-of-distribution (OOD) data. By keeping the test conditions constant while varying the models, we can isolate the effect of model architecture and training on their ability to adapt to novel inputs through in-context learning.

## 4 Transformer abilities to in-context learn mathematical functions

### 4.1 Models can ICL<sub>1</sub> polynomial functions of degree > 1

We consider the ICL problem for the function classes  $\mathbb{R}^n[X]$ , consisting of polynomials of degree  $n \leq 6$ , with both input samples and weights sampled uniformly from the interval  $[-1, 1]$ ; that is  $\mathcal{D}_{\mathcal{I}} = \mathcal{D}_{\mathcal{F}} = \mathcal{U}(-1, 1)$ .

Our experiments show that all tested models can successfully ICL<sub>1</sub> this task. Our models match the performance of classical polynomial regression techniques, such as Least Squares, which are known to achieve optimal recovery when the degree of the polynomial is known. For each polynomial degree up to six, the transformers consistently attain low mean squared error when  $\mathcal{D}_{\mathcal{I}}^{test} = \mathcal{D}_{\mathcal{F}}^{test} = \mathcal{U}(-1, 1)$ , as shown in Figure 3 and detailed in Tables 2 and 3. Moreover, an analysis of the attention

<sup>1</sup>Our code can be found in <https://anonymous.4open.science/r/icl-polynomials/>

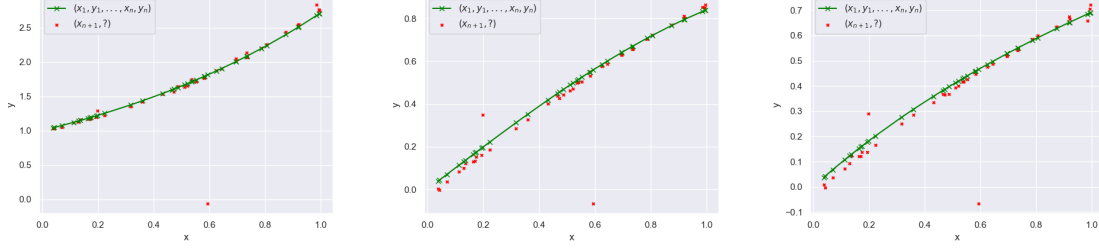


Figure 1: ICL of  $e^x$ ,  $\sin(x)$  and  $\ln(1+x)$  on  $[0, 1]$  by a model trained on  $\mathbb{R}^3[X]$ .

weights at all 12 layers in our best models showed remarkably similar patterns, regardless of the complexity of the polynomial being computed and that the resolution of the ICL problem took place mainly in the last layer (Figure 8 in Appendix F).

**Proposition 1.** *Transformer models can  $ICL_1$  polynomial functions when  $D_{\mathcal{T}} = D_{\mathcal{F}} = D_{\mathcal{T}}^{test} = D_{\mathcal{F}}^{test} = \mathcal{U}[-1, 1]$  in line with optimal algorithms.*

**Observation 1.** *All models had roughly the same error rates for each polynomial class  $\mathbb{R}^n[X]$ , for as high as we tested.*

## 4.2 Training on polynomial functions suffices to ICL some continuous functions

The results on polynomials have an important consequence. According to the Stone-Weierstrass theorem, any continuous function on an interval  $[a, b]$  can be uniformly approximated as closely as desired by a polynomial function. In other words, sufficiently high degree polynomials can mimic any continuous function with high accuracy.

**Proposition 2.** *If a transformer model can  $ICL_1$  a class  $\mathbb{R}^n[X]$ , then it can  $ICL_1$  a continuous function  $f$  over an interval  $[a, b]$  that has an expansion in terms of  $\mathbb{R}^n[X]$*

Despite being trained only on polynomials of degree  $\leq n$  and with just a few prompts of the form  $(x, f(x))$ , our models achieve low approximation error on smooth continuous functions not seen during training, including smooth functions with known Taylor expansions (e.g.,  $\exp(x)$ ,  $\sin(x)$ ,  $\log(1+x)$ ) as well as non-smooth functions such as  $|x|$ , confirming their ability to generalize based on polynomial structure (see Figures 1 and 6).

## 4.3 Transformers can generalize to unseen classes of polynomial functions

In this section, we investigate a generalization ability of transformers to ICL functions from a class not seen in training. We consider three approaches

to training. The first approach restricts the training data to polynomials of a fixed degree  $n$ . This setup serves as a baseline to assess the model’s performance when trained on a single degree class. The second approach adopts a curriculum learning on polynomial degrees, where the model is progressively exposed to polynomials of increasing degree starting with degree 1, to degree  $n$ . This method aims to facilitate learning by gradually increasing the difficulty of the training examples. The third approach explores the model’s capacity for generalization with a training regime in which there are gaps in the classes of polynomials seen in training. In particular, we train on polynomials of degrees 1, 3, and 5, without training on degrees 2 and 4. This setting allows us to evaluate the model’s ability to interpolate or extrapolate across unseen degrees.

The training strategy that yielded the best generalization performance involved exposing the model to polynomials of degrees 1, 3, and 5, while deliberately excluding degrees 2 and 4. Transformer models with this training, both with and without an MLP component, exhibited performance on unseen degrees comparable to models fully trained on these degrees. Indeed we found that the attention layers were both necessary and sufficient for ICL, with MLP only models unable to ICL. This reflects (Mickus et al., 2022)’s findings on the importance of attention layers for various NLP tasks. Figure 2 depicts the results across polynomial classes. The observed improvement in generalization indicates that introducing gaps between degrees in the training data may encourage the model to learn more robust representations, potentially capturing underlying structures that generalize better across the entire space of polynomial functions. More generally, it suggests that for transformers to learn generalizable representations it may be desirable to omit information in training so that they can infer this information.



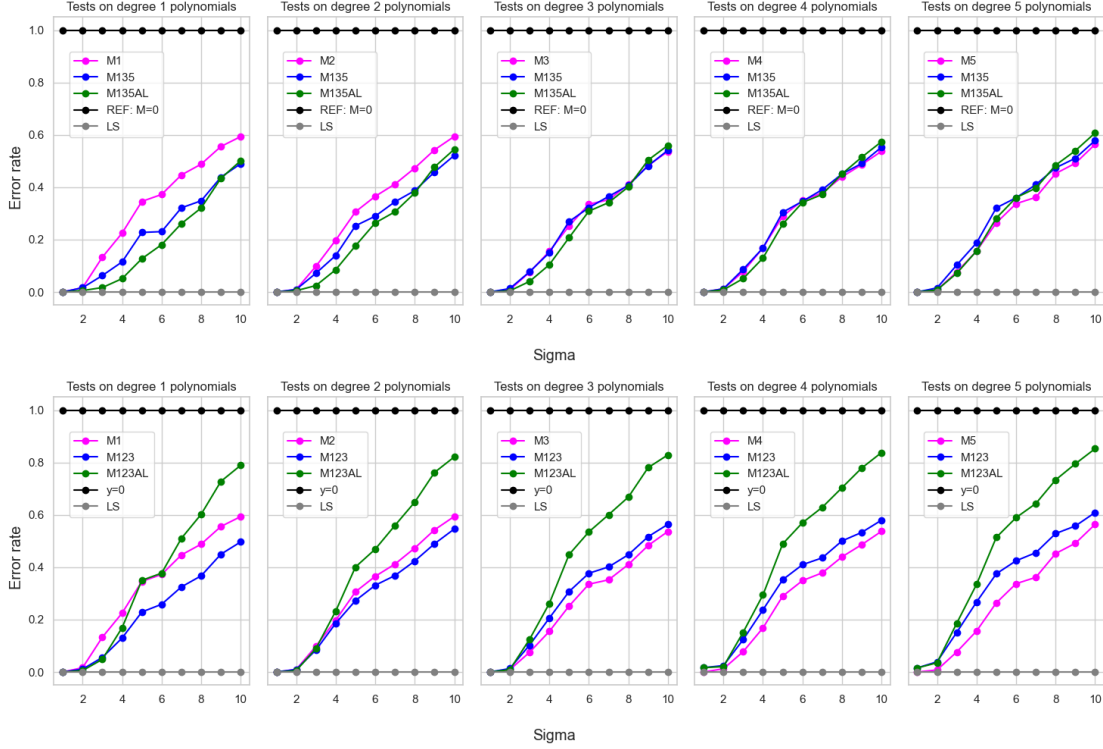


Figure 2: First line of graphs gives error rates for M135, a full 12L8AH transformer model trained on degrees 1,3 and 5 with values and inputs sampled from  $\mathcal{U}(-1, 1)$ , Mn the same model trained only on degree  $n$  and M135AL, a 12L8AH model with only attention layers and no MLP layers. All models were tested on polynomials of degrees 1-5. Second line gives similar results for models trained by curriculum on degrees 1,2 and 3.

## 5 Limitations and analysis

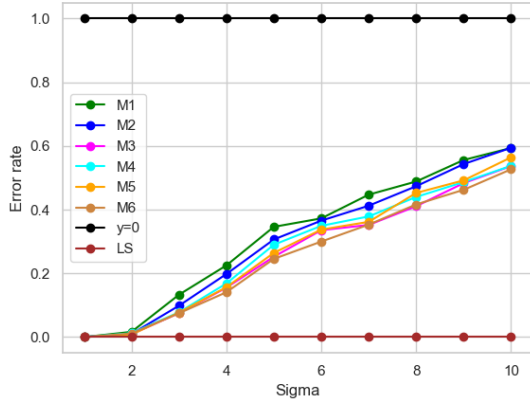


Figure 3: Evolution of error rates for various 12L8AH  $d_{emb} = 256$  models with  $D_{\mathcal{F}}, D_{\mathcal{I}} = D_I^t = \mathcal{U}(-1, 1)$  and  $D_{\mathcal{F}}^t$  for various  $\mathcal{U}(-\sigma, \sigma)$  trained from scratch, each on a different degree. E.g., Mn is a model trained on degree  $n$  only. The black line illustrates a model that predicts  $f(x_n) = 0, \forall f$  and  $\forall x_n$ . The dark red line LS represents a perfect estimator given our totally clean input data.

Our models behaved remarkably similarly on

ICL problems with different types of polynomial functions and continuous functions. They did not need the class forms or the degree of the functions they were approximating. In this sense, our models did better than optimal algorithms like LS or polynomial regression, which require knowing a function’s degree.

However, although all models performed nearly perfectly when test distributions closely matched training distributions (i.e.,  $D_{\mathcal{F}}^{test} \approx D_{\mathcal{F}}$  and  $D_{\mathcal{I}}^{test} \approx D_{\mathcal{I}}$ ), their performance deteriorated significantly as the test distributions deviated from the training regime. This indicates model sensitivity to shifts in both  $D_{\mathcal{I}}$  and  $D_{\mathcal{F}}$ , as illustrated in Figure 3 and in the heatmap in Figure 7. Our findings<sup>2</sup> on higher order polynomial and continuous functions echo those of (Naim and Asher, 2024) for linear functions. Notably, increasing model size from 22.5M to 38M parameters did not significantly improve performances, suggesting that the observed limitations are not simply due to model capacity but may reflect deeper architectural constraints.<sup>3</sup>

<sup>2</sup>See Figure 5 for results for training and testing with Gaussian distributions  $\mathcal{N}(0, \sigma)$ .

<sup>3</sup>by taking  $d_{emb} = 512$  instead of  $d_{emb} = 256$ .

(Naim and Asher, 2024) reported that models trained on linear functions exhibit limit values they cannot exceed, constraining their generalization ability: *boundary values*. We observe similar behavior in all our models trained on polynomial functions: they can perform in-context learning (ICL) up to a certain threshold, beyond which generalization breaks down for large input values. This behavior is clearly illustrated in Figure 4. As a result, and as shown in Figure 3, the error rate increases progressively as we move further away from the training distribution.

Training with distributions over much larger intervals, for instance<sup>4</sup>  $\mathcal{U}(-100, 100)$ , can extend boundary values. However, as shown in Table 3, such training comes at a substantial cost: performance deteriorates sharply across all testing scenarios we considered.

To investigate the cause of boundary values, we did an ablation study. We first remove MLP from transformer architecture. Models without MLP still performed well on ICL tasks, reaffirming prior findings that attention is the primary mechanism enabling in-context learning (Olsson et al., 2022; Naim and Asher, 2024). However, these models continued to exhibit boundary values, indicating that the issue is not caused by the MLP.

A more revealing result emerged when the normalization layer was removed: the model began producing significantly larger output values, effectively eliminating the boundary values observed previously. This behavior indicates that layer normalization acts as the principal mechanism enforcing a hard predictive threshold. By constraining the magnitude of internal activations, it prevents the model from extrapolating beyond the range seen during training, thereby limiting generalization, especially in high-input regimes.

We expected a significant drop in performance upon removing layer normalization (Ba et al., 2016), given its established role in reducing internal covariate shift and stabilizing training dynamics (Dai et al., 2023; Mueller et al., 2023). However, somewhat surprisingly, we observe improved results when the input and function distributions are set to  $D_{\mathcal{I}} = D_{\mathcal{F}} = \mathcal{U}(-1, 1)$  (Table 1). We attribute this behavior to the controlled nature of this regime: the input values lie within  $[-1, 1]$  a compact, symmetric interval centered at zero, where the variance

and scale of inputs are inherently stable. In such a setting, the primary motivation for normalization, which is handling shifts in activation statistics, is largely irrelevant.

Without layer normalization, the model can produce outputs that exceed the usual boundary values seen with normalization. As a result, the model is able to approximate certain functions more accurately, especially near the boundaries of the input domain, where layer normalization would otherwise constrain the output. Thus, we predict removing normalization in our controlled regime where issues like internal covariate shift are unlikely to arise, improves scores. Removing normalization may improve a model’s representational capacity in similar situations. However, even if the model can approximate large values without LN, the model still couldn’t  $ICL_2$  as Table 1 indicates for big values.

**Observation 2.** *Transformers without normalization can achieve better performance.*

## 6 A closer look at in-context learning

A transformer is a neural network model that maps a sequence of input vectors  $(x_1, \dots, x_n)$  to a corresponding sequence of output vectors, through a stack of layers. Each layer in the transformer operates on a sequence of vectors  $X^{(l)} = (x_1^{(l)}, x_2^{(l)}, \dots, x_n^{(l)})$ , which represents the sequence at layer  $l$ , and produces a new matrix  $X^{(l+1)}$  for the next layer.

We focus on the case of autoregressive, decoder-only transformer model composed of  $L$  layers and  $H$  attention heads. In each layer, the input sequence is first processed by a multi-head self-attention mechanism. Each attention head computes attention weights and context vectors independently. The attention head operation is defined as:

$$(x_1^{(l)}, \dots, x_n^{(l)}) \rightarrow (A^{h,(l+1)}(x_1^{(l)}), \dots, A^{h,(l+1)}(x_n^{(l)}))$$

where  $\forall i \in \{1, \dots, n\}$

$$A^{h,(l+1)}(x_i^{(l)}) = \sum_{j=1}^n s \left( x_i^{(l)} (Q^h K^{hT}) x_j^{(l)T} \right) x_j^{(l)} V^h \quad (4)$$

with  $Q^h \in \mathbb{R}^{d_{model} \times d_q}$ ,  $K^h \in \mathbb{R}^{d_{model} \times d_k}$  and  $V^h \in \mathbb{R}^{d_{model} \times d_v}$  are Query, Key and Value matrices with  $d_q = d_k = d_v = d_{model}/h$  and  $s$  is the scoring function.

The outputs of attention heads are concatenated

<sup>4</sup>For illustrations see Appendix E and with models with Hard max instead of softmax (Giannou et al., 2024).

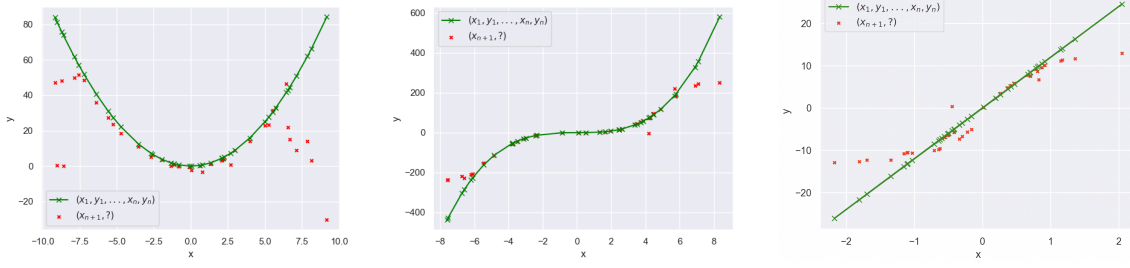


Figure 4: First two plots for models  $P2$  for  $f(x) = x^2$   $P3$  for  $f(x) = x^3$ , trained on  $D_{\mathcal{I}} = D_{\mathcal{F}} = N(0, 1)$  showing boundary values. Third plot shows boundary values for 2L32ah attention only model, with  $d_{embedding} = 256$  to ICL the function  $f(x) = 12x$ .

models \ $\sigma$	1	2	3	4	5	6	7	8	9	10
With LN	$3.5 \times 10^{-5}$	0.03	0.55	1.37	4.0	5.17	9.04	12.07	19.28	27.85
Without LN	$9.7 \times 10^{-6}$	$3 \times 10^{-3}$	0.16	0.81	2.99	3.37	7.52	10.92	17.40	25.44

Table 1: Comparison showing the evolution of squared errors for models trained on degree 1 on different distributions  $D_{\mathcal{I}} = D_{\mathcal{F}} = \mathcal{U}(-1, 1)$ , and tested on  $D_{\mathcal{I}}^t = \mathcal{U}(-1, 1)$  and  $D_{\mathcal{F}}^t = \mathcal{U}(-\sigma, \sigma) \forall \sigma \in \{1, \dots, 10\}$ , with and without layer normalization.

then passed through a linear layer to form the output of the multi-head attention mechanism :

$$(A^{(l+1)}(x_1^{(l)}), \dots, A^{(l+1)}(x_n^{(l)}))$$

where  $\forall i \in \{1, \dots, n\}$

$$A^{(l+1)}(x_i^{(l)}) = \sum_{h=1}^H A^{h,(l+1)} \gamma_h(x_i^{(l)})$$

with  $\gamma_h \in \mathbb{R}^{d_v \times d}$  are the weights of the linear layer. The output of the multi-head attention module is then passed through the *Add & Norm* operation. The result  $\forall i \in \{1, \dots, n\}$  is:

$$AN_i^{(l+1)} = LN(A^{(l+1)}(x_i^{(l)}) + x_i^{(l)})$$

The normalized output is then passed through a feedforward network:

$$W_1^{(l+1)} \sigma \left( W_2^{(l+1)} AN_i^{(l+1)} \right)$$

The output of the feedforward network is then passed through another *Add & Norm* operation to produce the final output of the layer  $l + 1$ :

$$LN \left( W_1^{(l+1)} \sigma \left( W_2^{(l+1)} AN_i^{(l+1)} \right) + AN_i^{(l+1)} \right)$$

The transformer, denoted by  $\hat{f}^\theta$  processes the ICL input of the form  $(x_1, g(x_1), \dots, x_p, g(x_p), x)$ , and produces a prediction  $\hat{f}^\theta(x_1, g(x_1), \dots, x_p, g(x_p), x)$  after processing the inputs in  $L$  layers. Given the explicit form of  $\hat{f}^\theta$ , which operates autoregressively

over the input sequence, we can in principle express the output as a deterministic function of the entire prompt. This allows us to analyze and potentially characterize the model’s ICL behavior for any specific prompt configuration, making it possible to study whether and how it implicitly implements a learning algorithm over the in-context examples.

The explicit mathematical expression of  $\hat{f}^\theta$  yields several conclusions. First, the model output expression reflects a weighted combination of input tokens, governed by softmax-like attention scores. It does not resemble the application of any classical learning algorithm such as least squares, ridge regression, or interpolation. Even in the case of this relatively simple transformer setup, the resulting output for a query  $x$  is determined by a fixed pattern of operations (attention weighting followed by projection), rather than by an adaptive mechanism that infers a generalizable rule from the input-output pairs. This suggests that, rather than implementing a specific algorithm, the model applies a sequence of learned transformations over the prompt to approximate function values within certain boundary values. The observed degradation in performance when evaluating on inputs outside the training range, and the fact that attention weights remained remarkably similar during ICL predictions for functions with different degrees adds empirical support to our theoretical conclusion that the models do not infer and apply a global function form.

The explicit form of  $\hat{f}^\theta$  also yields a theoretical proof establishing the existence of boundary values in the model’s predictions. The full proof is presented in Appendix G.1.

**Proposition 3.** *Boundary values occur due to Layer Normalization*

While eliminating layer normalization successfully removes the boundary value effect, it does not enable the model to effectively ICL and adapt to in-context examples when the query input  $x$  has a large embedding norm. In this regime, the model’s output asymptotically converges to a linear function of the form  $\hat{f}^\theta(x_1, g(x_1), \dots, x) \approx_{||x|| \rightarrow \infty} ax + b$ , where  $a$  and  $b$  are set by the model’s fixed parameters during pretraining and are minimally affected by the in-context examples. (Appendix G.2). The model diverges toward unbounded outputs that fail to reflect the intended target  $g(x)$ . This behavior indicates that, in the absence of layer normalization, the model’s predictions become insensitive to the prompt content as  $||x||$  increases, thus precluding ICL.

Layer normalization constrains a model’s outputs to a bounded range to provide good performance, but it introduces the pathology of boundary value behavior. Thus:

**Proposition 4.** *Transformer models cannot perform in-context learning over inputs with high embedding norm.*

The softmax function used in the attention mechanism in Equation 4 also limits in-context learning. The explicit form of  $\hat{f}^\theta$  shows that the characteristics of softmax-based attention can significantly affect the model’s ability to generalize. The softmax function has two behaviors that limit its effectiveness in ICL. First, when one input value is significantly larger than the rest, softmax, like hardmax, assigns a probability close to 1 to the largest value and nearly zero to all others. This concentrates attention almost entirely on a single token, discarding the surrounding context. Second, when dealing with long sequences where the input values are both numerous and similar in magnitude, softmax tends to a uniform distribution. In such cases, it effectively averages across all tokens, blurring distinctions between relevant and irrelevant inputs (for details see Appendix G.2). These behaviors undermine the model’s ability to adaptively and selectively leverage in-context examples.

We draw three morals for general transformer use. First, while authors have examined trans-

former embeddings for interpretability (Dar et al., 2022; Mickus et al., 2022), our formal and empirical results show that embeddings should obey constraints to be optimal: avoid embeddings with a high norm and embeddings that create large norm differences between token embeddings. However, for problems like ours where the embedding has to respect exogenous constraints like the natural ordering on  $\mathbb{R}$ , it may be impossible to follow our suggestion. Finally, our results show that to improve long context comprehension and generation (Huang et al., 2023), revising a transformer’s scoring function is desirable.

## 7 Conclusion

Our study analyzes the limitations of in-context learning by using a controlled experimental setup based on polynomial function approximation. Polynomial functions offer a simple yet expressive framework to uncover key generalization behaviors. Our analysis reveals critical fundamental architectural limitations. Specifically, we find that components such as layer normalization and the softmax scoring function within attention impose structural constraints that limit generalization, especially under distribution shift or at the boundaries of the training regime.

Understanding both the strengths and weaknesses of ICL is essential, since modern systems especially in NLP rely heavily on few-shot prompting and generalization to unseen tasks and domains. The task complexity of NLP applications often hides or makes it difficult to interpret the failure modes our analysis has isolated and explained. But understanding these failure modes and ICL limits more generally is crucial to ensuring ICL’s success, as it becomes a key element in NLP applications like dialogue systems, knowledge extraction, and multi-agent communication.

## Limitations

While our study offers valuable insights into the structural limits of in-context learning (ICL) in transformer models, it comes with several limitations that open avenues for future research.

Our experiments use a controlled setting with synthetic mathematical functions. Although this setup enables a precise analysis of model behavior and architectural effects, it abstracts away from many complexities present in real-world NLP tasks, such as natural language variability, noise, and hier-



archical structure. As a result, we have only made one direct generalization to high-level language tasks concerning long context comprehension and generation in NLP.

Our analysis is primarily focused on decoder-only transformers with relatively modest model sizes (up to 38M parameters). While the mathematical results hold for all transformers, larger models used for instance in production NLP systems may very well exhibit less drastic limitations on generalization due to scale.

Despite these limitations, our framework and findings lay the groundwork for understanding and addressing ICL failure modes, offering a foundation for improved architectural design and training strategies in both synthetic and natural language domains.

## References

- Ekin Akyürek, Dale Schuurmans, Jacob Andreas, Tengyu Ma, and Denny Zhou. 2022. What learning algorithm is in-context learning? investigations with linear models. *arXiv preprint arXiv:2211.15661*.
- Jimmy Lei Ba, Jamie Ryan Kiros, and Geoffrey E Hinton. 2016. Layer normalization. *arXiv preprint arXiv:1607.06450*.
- Satwik Bhattamishra, Arkil Patel, Phil Blunsom, and Varun Kanade. 2023. Understanding in-context learning in transformers and llms by learning to learn discrete functions. *arXiv preprint arXiv:2310.03016*.
- Alberto Bietti, Vivien Cabannes, Diane Bouchacourt, Herve Jegou, and Leon Bottou. 2024. Birth of a transformer: A memory viewpoint. *Advances in Neural Information Processing Systems*, 36.
- Tom Brown, Benjamin Mann, Nick Ryder, Melanie Subbiah, Jared D Kaplan, Prafulla Dhariwal, Arvind Neelakantan, Pranav Shyam, Girish Sastry, Amanda Askell, and 1 others. 2020. Language models are few-shot learners. *Advances in neural information processing systems*, 33:1877–1901.
- Yan Dai, Kwangjun Ahn, and Suvrit Sra. 2023. The crucial role of normalization in sharpness-aware minimization. *Advances in Neural Information Processing Systems*, 36:67741–67770.
- Guy Dar, Mor Geva, Ankit Gupta, and Jonathan Berant. 2022. Analyzing transformers in embedding space. *arXiv preprint arXiv:2209.02535*.
- P Kingma Diederik. 2014. Adam: A method for stochastic optimization. (*No Title*).
- Qingxiu Dong, Lei Li, Damai Dai, Ce Zheng, Jingyuan Ma, Rui Li, Heming Xia, Jingjing Xu, Zhiyong Wu, Tianyu Liu, and 1 others. 2022. A survey on in-context learning. *arXiv preprint arXiv:2301.00234*.
- Deqing Fu, Tian-Qi Chen, Robin Jia, and Vatsal Sharan. 2023. Transformers learn higher-order optimization methods for in-context learning: A study with linear models. *arXiv preprint arXiv:2310.17086*.
- Shivam Garg, Dimitris Tsipras, Percy S Liang, and Gregory Valiant. 2022. What can transformers learn in-context? a case study of simple function classes. *Advances in Neural Information Processing Systems*, 35:30583–30598.
- Mor Geva, Jasmijn Bastings, Katja Filippova, and Amir Globerson. 2023. Dissecting recall of factual associations in auto-regressive language models. In *Proceedings of the 2023 Conference on Empirical Methods in Natural Language Processing*, pages 12216–12235.
- Mor Geva, Roei Schuster, Jonathan Berant, and Omer Levy. 2021. Transformer feed-forward layers are key-value memories. In *Proceedings of the 2021 Conference on Empirical Methods in Natural Language Processing*, pages 5484–5495.
- Angeliki Giannou, Liu Yang, Tianhao Wang, Dimitris Papailiopoulos, and Jason D Lee. 2024. How well can transformers emulate in-context newton’s method? *arXiv preprint arXiv:2403.03183*.
- Yunpeng Huang, Jingwei Xu, Junyu Lai, Zixu Jiang, Taolue Chen, Zenan Li, Yuan Yao, Xiaoxing Ma, Lijuan Yang, Hao Chen, and 1 others. 2023. Advancing transformer architecture in long-context large language models: A comprehensive survey. *arXiv preprint arXiv:2311.12351*.
- Timothee Mickus, Denis Paperno, and Mathieu Constant. 2022. How to dissect a muppet: The structure of transformer embedding spaces. *Transactions of the Association for Computational Linguistics*, 10:981–996.
- Maximilian Mueller, Tiffany Vlaar, David Rolnick, and Matthias Hein. 2023. Normalization layers are all that sharpness-aware minimization needs. *Advances in Neural Information Processing Systems*, 36:69228–69252.
- Omar Naim and Nicholas Asher. 2024. Re-examining learning linear functions in context. *ArXiv:2411.11465 [cs.LG]*.
- Catherine Olsson, Nelson Elhage, Neel Nanda, Nicholas Joseph, Nova DasSarma, Tom Henighan, Ben Mann, Amanda Askell, Yuntao Bai, Anna Chen, and 1 others. 2022. In-context learning and induction heads. *arXiv preprint arXiv:2209.11895*.
- Madhur Panwar, Kabir Ahuja, and Navin Goyal. 2023. In-context learning through the bayesian prism. *arXiv preprint arXiv:2306.04891*.
- Allan Raventós, Mansheej Paul, Feng Chen, and Surya Ganguli. 2024. Pretraining task diversity and the emergence of non-bayesian in-context learning for regression. *Advances in Neural Information Processing Systems*, 36.

Juergen Schmidhuber, Jieyu Zhao, and Marco Wiering. 1996. Simple principles of metalearning.

Johannes Von Oswald, Eyvind Niklasson, Ettore Randazzo, João Sacramento, Alexander Mordvintsev, Andrey Zhmoginov, and Max Vladymyrov. 2023. Transformers learn in-context by gradient descent. In *International Conference on Machine Learning*, pages 35151–35174. PMLR.

Jingfeng Wu, Difan Zou, Zixiang Chen, Vladimir Braverman, Quanquan Gu, and Peter L Bartlett. 2023. How many pretraining tasks are needed for in-context learning of linear regression? *arXiv preprint arXiv:2310.08391*.

Sang Michael Xie, Aditi Raghunathan, Percy Liang, and Tengyu Ma. 2021. An explanation of in-context learning as implicit bayesian inference. *arXiv preprint arXiv:2111.02080*.

Qinan Yu, Jack Merullo, and Ellie Pavlick. 2023. [Characterizing mechanisms for factual recall in language models](#). In *Proceedings of the 2023 Conference on Empirical Methods in Natural Language Processing*, pages 9924–9959, Singapore. Association for Computational Linguistics.

Yufeng Zhang, Fengzhuo Zhang, Zhuoran Yang, and Zhaoran Wang. 2023. What and how does in-context learning learn? bayesian model averaging, parameterization, and generalization. *arXiv preprint arXiv:2305.19420*.

## A Training details

**Additional training information:** We use the Adam optimizer (Diederik, 2014) , and a learning rate of  $10^{-4}$  for all models.

**Computational resources:** We used Nvidia A-100 GPUs to train the different versions of transformer models from scratch.

## B Error rates with Gaussian test and training distributions

## C Error progression for models trained on $\mathcal{U}(-1, 1)$ and tested on $\mathcal{U}(-\sigma, \sigma)$

See Tables 2 and 3

## D Graphs for ICL of $|x|$

See Figure 6

## E Model performance on a distribution depends on its density in Training

A key factor in generalization ability is the proportion of points from the test distribution that the model was exposed to during training relative to the total number of points encountered throughout

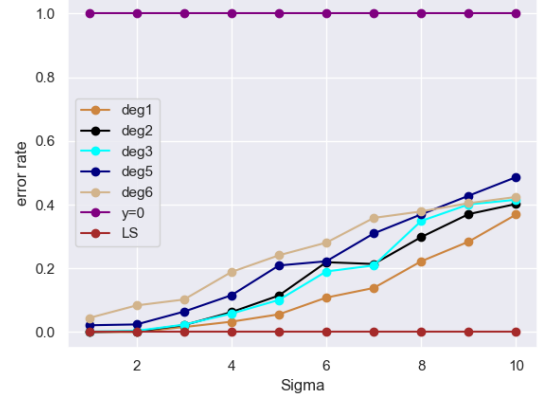


Figure 5: Evolution of error rates for various 12L8AH  $d_{emb} = 256$  models with  $D_{\mathcal{F}}, D_{\mathcal{T}} = D_I^t = N(0, 1)$  and  $D_F^t$  for various  $N(0, \sigma)$  trained from scratch on different degrees. The purple curves illustrate a model that predicts  $f(x_n) = 0, \forall f$  and  $\forall x_n$ . The dark red line LS represents a perfect estimator given our totally clean input data.

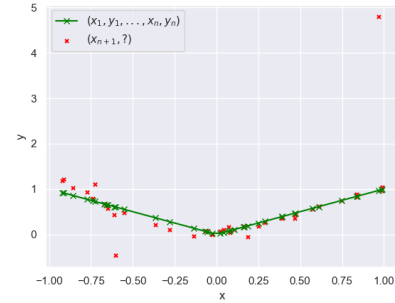


Figure 6: Plots for model  $P^3$  for the prediction of  $f(x)=|x|$

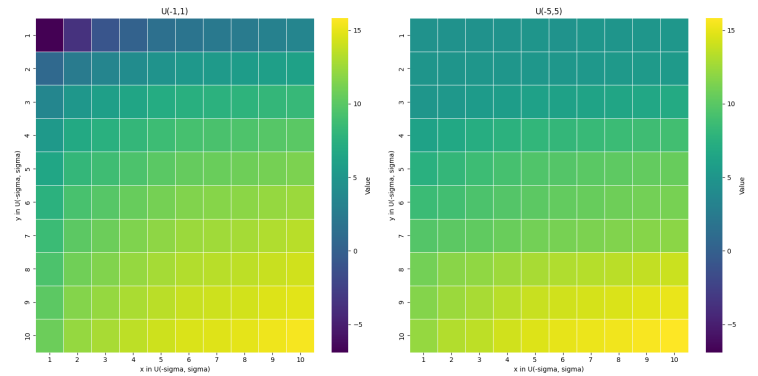


Figure 7: Heatmap showing evolution of log of squared error  $\epsilon$  with  $D_I^t = D_F^t = \mathcal{U}(-\sigma, \sigma)$  on polynomials of degree 3 for  $\sigma \in \{1, \dots, 10\}$  for the models M135, the left trained on  $D_{\mathcal{T}} = D_{\mathcal{F}} = \mathcal{U}(-1, 1)$  and the right on  $D_{\mathcal{T}} = D_{\mathcal{F}} = \mathcal{U}(-5, 5)$ .

the training process (Table 3) (Naim and Asher,

degree	models / $\sigma$	1	2	3	4	5	6	7	8	9	10
1	M1	0.0	0.03	0.55	1.37	4.0	5.17	9.04	12.07	19.28	27.85
	M135	0.0	0.03	0.26	0.7	2.63	3.2	6.5	8.61	15.21	<b>22.98</b>
	M135AL	0.0	<b>0.01</b>	<b>0.07</b>	<b>0.31</b>	<b>1.47</b>	<b>2.51</b>	<b>5.28</b>	<b>7.93</b>	<b>15.06</b>	23.52
	REF: $y=0$	0.46	1.84	4.14	6.09	11.56	13.88	20.22	24.72	34.69	46.92
2	M2	0.0	0.02	0.48	1.49	4.01	6.41	9.69	13.11	19.96	32.97
	M135	0.0	0.02	0.35	1.05	3.31	5.08	8.1	10.72	<b>16.84</b>	<b>28.95</b>
	M135AL	0.0	<b>0.01</b>	<b>0.12</b>	<b>0.64</b>	<b>2.31</b>	<b>4.63</b>	<b>7.2</b>	<b>10.47</b>	17.56	30.25
	REF: $y=0$	0.52	2.05	4.88	7.53	13.09	17.54	23.5	27.69	36.76	55.49
3	M3	0.0	0.02	0.41	1.25	3.69	6.77	9.12	12.14	19.34	<b>31.57</b>
	M135	0.0	0.03	0.42	1.21	3.94	6.5	9.46	12.03	<b>19.3</b>	31.84
	M135AL	0.0	<b>0.01</b>	<b>0.22</b>	<b>0.84</b>	<b>3.04</b>	<b>6.23</b>	<b>8.85</b>	<b>11.87</b>	20.17	32.94
	REF: $y=0$	0.56	2.27	5.45	8.06	14.64	20.18	25.91	29.56	40.03	58.81
4	M4	0.0	0.03	0.44	1.48	4.66	7.65	10.5	14.47	<b>20.36</b>	<b>32.94</b>
	M135	0.0	0.03	0.49	1.48	4.9	7.59	10.84	<b>14.83</b>	20.55	33.92
	M135AL	0.0	<b>0.02</b>	<b>0.29</b>	<b>1.14</b>	<b>4.17</b>	<b>7.49</b>	<b>10.33</b>	14.84	21.55	35.19
	REF: $y=0$	0.6	2.45	5.66	8.8	16.08	21.91	27.73	32.9	41.85	61.29
5	M5	0.0	0.02	0.46	<b>1.51</b>	<b>4.52</b>	<b>7.9</b>	<b>10.52</b>	<b>16.4</b>	<b>21.84</b>	<b>37.66</b>
	M135	0.0	0.04	0.62	1.81	5.5	8.43	11.93	17.19	22.69	38.66
	M135AL	0.0	<b>0.02</b>	<b>0.43</b>	<b>1.51</b>	4.83	8.44	11.54	17.56	23.97	40.58
	REF: $y=0$	0.64	2.57	6.0	9.65	17.11	23.42	29.09	36.25	44.41	66.77

Table 2: Comparison to show the evolution of squared error  $\epsilon$ , with  $D_{\mathcal{I}}^t = \mathcal{U}(-1, 1)$ ,  $D_{\mathcal{F}}^t = \mathcal{U}(-\sigma, \sigma)$  for models  $M1$ ,  $M135$  and  $M135AL$

models \ $\sigma$	1	2	3	4	5	6	7	8	9	10
$\mathcal{U}(-1, 1)$	0.0	0.03	0.55	1.37	4.0	5.17	9.04	12.07	19.28	27.85
$\mathcal{U}(-5, 5)$	0.01	0.01	0.02	0.03	0.03	0.05	0.12	0.27	0.75	1.61
$\mathcal{U}(-10, 10)$	0.13	0.15	0.17	0.2	0.26	0.26	0.32	0.35	0.41	0.49
$\mathcal{U}(-100, 100)$	2217.84	2373.82	2494.31	2526.93	2472.45	2467.52	2317.92	2232.03	2129.0	2092.81

Table 3: Comparison showing the evolution of squared errors for models trained on different distributions  $D_{\mathcal{I}} = D_{\mathcal{F}} = \mathcal{U}(-a, a)$ , for  $a = 1, 5$  or  $100$  sampling from  $\mathcal{P}^1$  with  $D_{\mathcal{I}}^t = \mathcal{U}(-1, 1)$  and  $D_{\mathcal{F}}^t = \mathcal{U}(-\sigma, \sigma)$ .

2024).

**Observation 3.** (i) Models have better performance over intervals that contain a larger proportion of examples in the training distribution. (ii) Models trained on a distribution with larger variance (up to a certain point) had better generalization ability but less accuracy than models trained on distributions with smaller variance.

## F Evolution of predictions over layers

Evolution of predictions over layers show that the final prediction is mainly generated in the last layer. This behavior remains the same for all models tested.

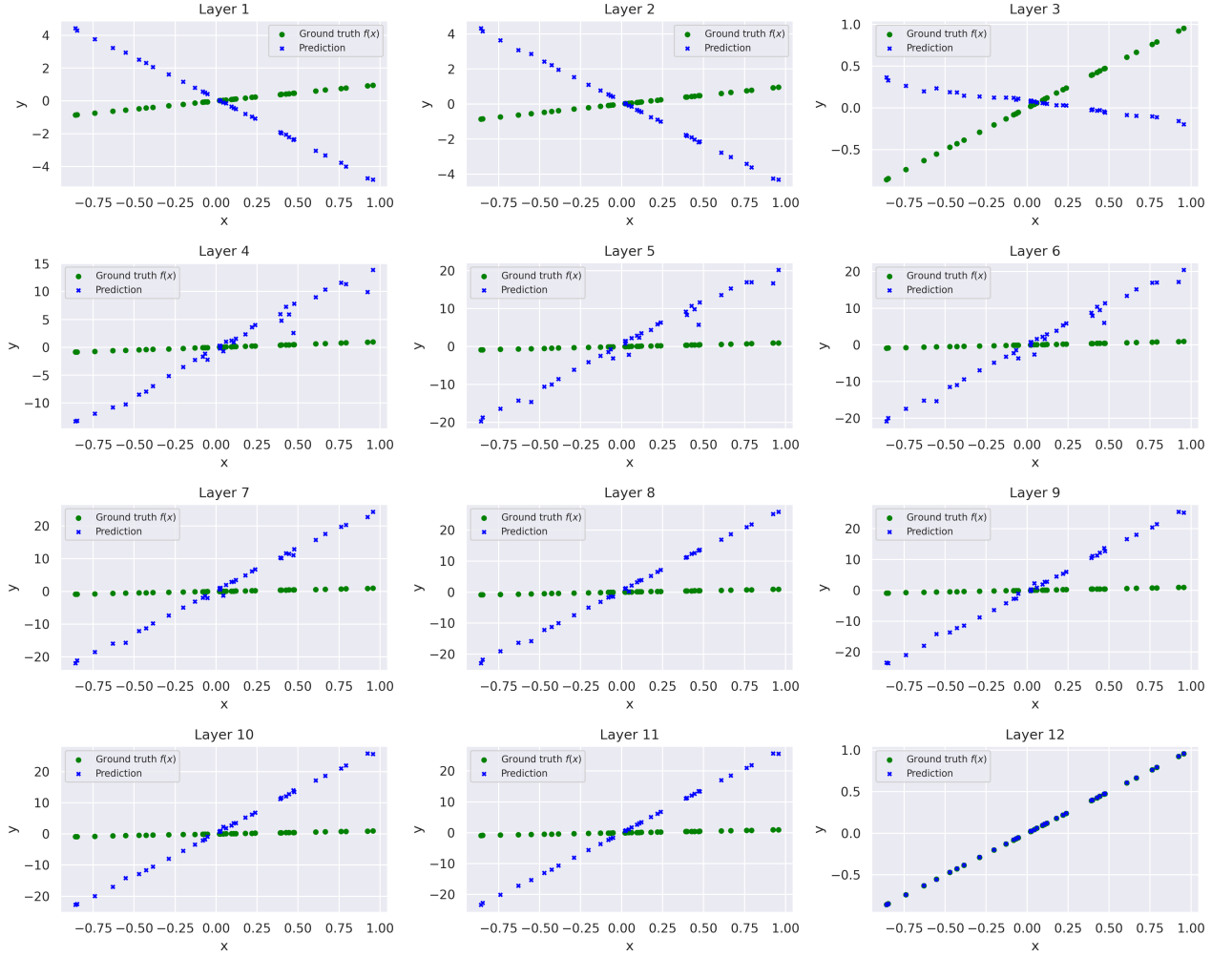


Figure 8: Plots showing evolution of the predictions over layers for  $f(x) = x$  for a model trained on degree 1 with  $D_{\mathcal{I}} = D_{\mathcal{F}} = \mathcal{U}(-1, 1)$ . Predictions are mainly generated in the last layer.



## G Proof for Boundary values

We consider of a transformer decoder only with  $n$  layers  $h$  attention heads  $\hat{f}_\theta$ . During ICL the model processes the ICL input of the form  $(x_1, g(x_1), \dots, x)$  to produces a prediction  $\hat{f}^\theta(x_1, g(x_1), \dots, x_n, g(x_n), x)$ . We fix the context  $(x_1, g(x_1), \dots, x_p)$  and consider the function  $\hat{f}_p : x \rightarrow \hat{f}^\theta(x_1, g(x_1), \dots, x_p, g(x_p), x)$ . To simplify notations for the proof, we will call the context  $(x_1, g(x_1), \dots, x_n, g(x_n)) = (x_1, \dots, x_p)$

### G.1 Layer Normalization

Attention only transformer models showed capacities of ICL and has performances similar to transformers with MLP. So, in the following proof, we will consider a model of attention only.

The output of Multi-head attention can be written as :

$$Attn_{x_1, \dots, x_p}(x) = \sum_{h=1}^H \left( \sum_{j=1}^p s \left( \tilde{x}(Q^h K^{hT}) \tilde{x}_j^T \right) \tilde{x}_j + s \left( \tilde{x}(Q^h K^{hT}) x^T \right) \tilde{x} \right) V^h \gamma_h$$

Let's call  $\tilde{x}_i = x_i W$  the linear embedding corresponding to  $x$ , used in the training.

$$Attn_{x_1, \dots, x_p}(x) = \sum_{h=1}^H \left( \sum_{j=1}^p s \left( x x_j (W Q^h K^{hT} W^T) \right) x_j + s \left( x^2 (W Q^h K^{hT} W^T) \right) x \right) W V^h \gamma_h \quad (5)$$

**Proposition 5.** *The multihead attention function in the ICL set-up is asymptotically equivalent to a linear function  $x \rightarrow ax + b$*

By replacing the scoring function  $s$ :

$$Attn_{x_1, \dots, x_p}(x) = \sum_{h=1}^H \left( \sum_{j=1}^p \frac{x_j e^{x x_j (W Q^h K^{hT} W^T)}}{e^{x^2 (W Q^h K^{hT} W^T)} + \sum_{k=1}^p e^{x x_k (W Q^h K^{hT} W^T)}} + \frac{x e^{x^2 (W Q^h K^{hT} W^T)}}{e^{x^2 (W Q^h K^{hT} W^T)} + \sum_{k=1}^p e^{x x_k (W Q^h K^{hT} W^T)}} \right) W V^h \gamma_h$$

For simplification, let's note  $\alpha_h = W Q^h K^{hT} W^T \in \mathbb{R}$  et  $\zeta_h = W V^h \gamma_h \in \mathbb{R}^d$

We then have:

$$Attn_{x_1, \dots, x_p}(x) = \sum_{h=1}^H \left( \sum_{j=1}^p \frac{x_j e^{x x_j \alpha_h}}{e^{x^2 \alpha_h} + \sum_{k=1}^p e^{x x_k \alpha_h}} + \frac{x e^{x^2 \alpha_h}}{e^{x^2 \alpha_h} + \sum_{k=1}^p e^{x x_k \alpha_h}} \right) \zeta_h \quad (6)$$

Let's call  $\mu_j^h : x \rightarrow \frac{x_j e^{x x_j \alpha_h}}{e^{x^2 \alpha_h} + \sum_{k=1}^p e^{x x_k \alpha_h}}$  and  $\beta^h : x \rightarrow \frac{x e^{x^2 \alpha_h}}{e^{x^2 \alpha_h} + \sum_{k=1}^p e^{x x_k \alpha_h}}$

$$Attn_{x_1, \dots, x_p}(x) = \sum_{h=1}^H \left( \sum_{j=1}^p \mu_j^h(x) + \beta^h(x) \right) \zeta_h \quad (7)$$

to see the behavior of the function at infinity, we define the following sets

$\mathbb{H}^- = \{h \in \{1, \dots, H\} : \alpha_h < 0\}$ ,  $\mathbb{H}^+ = \{h \in \{1, \dots, H\} : \alpha_h > 0\}$  and  $\mathbb{H}^0 = \{h \in \{1, \dots, H\} : \alpha_h = 0\}$

$\mathbb{X}^+ = \{j \in \{1, \dots, p\} : x_j > 0\}$ ,  $\mathbb{X}^- = \{j \in \{1, \dots, p\} : x_j < 0\}$  and  $\mathbb{X}^0 = \{j \in \{1, \dots, p\} : x_j = 0\}$

We have then:

$$\begin{aligned} \text{Attn}_{x_1, \dots, x_p}(x) &= \sum_{h \in \mathbb{H}^+ \cup \mathbb{H}^- \cup \mathbb{H}^0} \left( \sum_{j \in \mathbb{X}^+ \cup \mathbb{X}^- \cup \mathbb{X}^0} \mu_j^h(x) + \beta^h(x) \right) \zeta_h \\ \text{Attn}_{x_1, \dots, x_p}(x) &= \sum_{h \in \mathbb{H}^+} \left( \sum_{j \in \mathbb{X}^+} \mu_j^h(x) + \beta^h(x) + \sum_{j \in \mathbb{X}^-} \mu_j^h(x) + \beta^h(x) + \sum_{j \in \mathbb{X}^0} \mu_j^h(x) + \beta^h(x) \right) \zeta_h \cdot L \\ &\quad + \sum_{h \in \mathbb{H}^-} \left( \sum_{j \in \mathbb{X}^+} \mu_j^h(x) + \beta^h(x) + \sum_{j \in \mathbb{X}^-} \mu_j^h(x) + \beta^h(x) + \sum_{j \in \mathbb{X}^0} \mu_j^h(x) + \beta^h(x) \right) \zeta_h \cdot L \\ &\quad + \sum_{h \in \mathbb{H}^0} \left( \sum_{j \in \mathbb{X}^+} \mu_j^h(x) + \beta^h(x) + \sum_{j \in \mathbb{X}^-} \mu_j^h(x) + \beta^h(x) + \sum_{j \in \mathbb{X}^0} \mu_j^h(x) + \beta^h(x) \right) \zeta_h \cdot L \end{aligned}$$

When  $x \rightarrow +\infty$ , the first sum  $S_1 \rightarrow_{x \rightarrow +\infty} x \sum_{\mathbb{H}^+} \zeta_h$ , the second  $S_2 \rightarrow_{x \rightarrow +\infty} \sum_{\mathbb{H}^-} (\sum_{j \in \mathbb{X}^-} \frac{x_j}{p} + x \sum_{j \in \mathbb{X}^0}) \zeta_h$  and the third sum:  $S_3 \rightarrow_{x \rightarrow +\infty} \sum_{\mathbb{H}^0} (\sum_{j=1}^p \frac{x_j}{p+1} + x \sum_{j=1}^p \frac{1}{p+1}) \zeta_h$

Finally  $\text{Attn}_{x_1, \dots, x_p}(x) \rightarrow_{x \rightarrow +\infty} Ax + B$

In the opposite, when  $x \rightarrow -\infty$ , with the same reasoning and it will tend asymptotically towards a linear function too.

**Proposition 6.** *Layer Normalization is responsible for boundary values*

The output after Multi-head attention  $\text{Attn}_{x_1, \dots, x_p}(x)$  is passed through the *Add & Norm* :

$$LN(\text{Attn}_{x_1, \dots, x_p}(x) + xW) = \frac{(\text{Attn}_{x_1, \dots, x_p}(x) + xW) - \text{mean}((\text{Attn}_{x_1, \dots, x_p}(x) + xW))}{\sqrt{\text{Var}(\text{Attn}_{x_1, \dots, x_p}(x) + xW)}} \rho + \epsilon$$

We will call  $\hat{\zeta}_h = \zeta_h - \text{mean}(\zeta_h)$  and  $\hat{W} = W - \text{mean}(W)$

In one hand,

$$((\text{Attn}_{x_1, \dots, x_p}(x) + xW)) - \text{mean}((\text{Attn}_{x_1, \dots, x_p}(x) + xW)) = \sum_{h=1}^H \left( \sum_{j=1}^p \mu_j^h(x) + \beta^h(x) \right) \hat{\zeta}_h + x\hat{W}$$

In the other hand,

$$\begin{aligned} \text{Var}(\text{Attn}_{x_1, \dots, x_p}(x) + xW) &= \frac{1}{d} \sum_{i=1}^d [\text{Attn}_{x_1, \dots, x_p}(x) + xW)_i - \text{mean}(\text{Attn}_{x_1, \dots, x_p}(x) + xW)]^2 \\ &= \frac{1}{d} \sum_{i=1}^d \left[ \sum_{h=1}^H \left( \sum_{j=1}^p (\mu_j^h(x) + \beta^h(x)) ((\zeta_h)_i - \text{mean}(\zeta_h)) \right) + x(W_i - \text{mean}(W)) \right]^2 \end{aligned}$$

By the same reasoning the variance  $\text{Var}(\text{Attn}_{x_1, \dots, x_p}(x) + xW) \rightarrow_{x \rightarrow \infty} c|x|$  as the nominator tends asymptotically towards a linear function at infinity it means that the ratio tends towards a constant that we have called boundary values. Although the mathematical reasoning speaks of infinity but this value appears immediately empirically

## G.2 Softmax

The softmax operation leads to context-independent outputs when there is a significant gap between values, causing it to behave like a hardmax, or when the number of tokens is large, in which case it approaches uniform averaging. This limitation is illustrated in Table 4.

Vector values	Softmax	Vector values	Softmax	Vector values	Softmax
1	0.192046	100	0.000045	1000	0
1.02	0.195925	102	0.000333	1020	0
1.03	0.197894	103	0.000905	1030	0
1.05	0.201892	105	0.006684	1050	0
1.1	0.212243	110	0.992033	1100	1

Table 4: Table showing that for large values, softmax performs like hardmax